

GEANT4 BASED MONTE CARLO SIMULATION FOR CARBON
FRAGMENTATION IN NUCLEAR EMULSION

A THESIS SUBMITTED TO
THE GRADUATE SCHOOL OF NATURAL AND APPLIED SCIENCES
OF
MIDDLE EAST TECHNICAL UNIVERSITY

BY

NAVID HOSSEINI

IN PARTIAL FULFILLMENT OF THE REQUIREMENTS
FOR
THE DEGREE OF MASTER OF SCIENCE
IN
PHYSICS

JULY 2012

Approval of the thesis:

**GEANT4 BASED MONTE CARLO SIMULATION FOR CARBON
FRAGMENTATION IN NUCLEAR EMULSION**

Submitted by **NAVID HOSSEINI** in partial fulfillment of the requirements for the degree of **Master of Science in Physics Department, Middle East Technical University** by;

Prof. Dr. Canan Özgen
Dean, Graduate School of **Natural and Applied Sciences**

Prof Dr. Mehmet T. Zeyrek
Head of Department, **Physics**

Prof Dr. Ali Murat Güler
Supervisor, **Physics Dept., METU**

Examining Committee Members:

Prof. Dr. Ramazan Sever
Physics Dept., METU

Prof. Dr. Ali Murat Güler
Physics Dept., METU

Prof. Dr. Orhan Çakır
Physics Dept., Ankara University

Prof. Dr. Bayram Tekin
Physics Dept., METU

Assist. Prof. Dr. Alpan Bek
Physics Dept., METU

Date: **06/07/2012**

I hereby declare that all information in this document has been obtained and presented in accordance with academic rules and ethical conduct. I also declare that, as required by these rules and conduct, I have fully cited and referenced all material and results that are not original to this work.

Name, Last name: Navid Hosseini

Signature:

ABSTRACT

GEANT4 BASED MONTE CARLO SIMULATION FOR CARBON FRAGMENTATION IN NUCLEAR EMULSION

Hosseini, Navid

M.S., Department of Physics

Prof. Dr. Ali Murat Güler

July 2012, 50 pages

The study is mainly focused on Monte Carlo simulation of carbon fragmentation in nuclear emulsion. The carbon ion is selected as a remarkable candidate for the cancer therapy usages due to its high efficiency in depositing majority of its energy in the narrow region which is called Bragg Peak. On the other hand, the main side effect of heavy-ion therapy is the radiation dose beyond the Bragg Peak which damages the healthy tissues. Therefore the use of heavy-ion in cancer therapy requires accurate understanding of ion-matter interactions which result in the production of secondary particles. A Geant4 based simulation of carbon fragmentation has been done considering 400 MeV/n carbon beam directed to the detector which is made of nuclear emulsion films, interleaved with lexan layers. Four different models in Geant4 are compared with recent real data. Among the four different models, Binary Cascade Model (BIC) shows a better agreement with real data.

Keywords: Bragg Peak, LET, Geant4, ECC, Monte Carlo

ÖZ

NÜKLEER EMÜLSİYONDAKİ KARBON PARÇALANMASININ GEANT4 MONTE CARLO SİMÜLASYONU

Hosseini, Navid

Yüksek Lisans, Fizik Bölümü

Tez Yöneticisi : Prof. Dr. Ali Murat Güler

Temmuz 2012, 50 sayfa

Bu çalışma, nükleer emülsiyon içerisinde karbon parçalanmasına odaklanmıştır. Karbon iyonunun kanser tedavisinde tercih edilmesinin sebebi enerjisinin çoğunu yüksek verimlilikle Bragg tepe noktasında depolamasındandır. Diğer taraftan ağıriyon terapide en önemli yan etki Bragg tepe noktasının arkasına sarkan radyasyon dozudur. Dolayısıyla kanser tedavisinde, ağır iyon kullanımı ikincil parçacıkların üretilmesine neden olan ağır iyon-madde etkileşimlerinin doğru anlaşılmasını gerektirir. Nükleer emülsiyon ve lexan plakalarından oluşan bir dedektöre yönlendirilen 400 MeV/n enerjili karbon iyonunun parçalanmasının simülasyonu Geant4 kullanılarak yapılmıştır. Geant4'deki dört farklı model yeni verilerle karşılaştırıldı. Bu dört model içerisinde Binary Cascade model verilerle en tutarlı olanıdır.

Anahtar Kelimeler: Bragg tepe noktasının, LET, Geant4, ECC, Monte Carlo

To My Parents and love

ACKNOWLEDGEMENT

I wish to express my sincerest gratitude to Prof. Dr. Ali Murat GÜLER for his kind supervision, invaluable support, friendship and help during my study.

Moreover, I would like to express my appreciation to Prof. Dr. Luciano Pandola, Prof. Dr. Giovanni De Lellis and Dr. Chiara Sirignano for their valuable comments and suggestions throughout the study.

A special gratitude goes to my friend Timur Dzhatdov from Moscow-Russia who has always found in assistance to me.

I also express my gratitude to Sohrab Gheibie and Suat Dengiz for their helps during my study.

I am grateful to all members of my great family: my mother Farideh, my father Latif, my sister Nava, for their continual encouragement and support in every stage of the entire of my life.

I would like to thank the Scientific and Technical Research Laboratory of Italy (INFN) for providing financial support for carrying out this research.

Finally, I want deeply dedicate my sincerest gratitude to my love, Arezoo for her continual love and support. It would not be possible for me to achieve this goal without her patience, understanding and unconditional support.

TABLE OF CONTENTS

ABSTRACT	iv
ÖZ.....	v
ACKNOWLEDGEMENT.....	vii
TABLE OF CONTENTS	viii
LIST OF FIGURES.....	x
CHAPTERS	
1.INTRODUCTION	
1.1 Clinical application of carbon ions and carbon therapy methods.....	2
1.2 Radiation therapy and carbon ion therapy advantageous	2
2.GEANT4 TOOLKIT FOR MONTE CARLO SIMULATIONS.....	4
2.1 Software facilities	4
2.2 Geant4 kernel.....	5
2.3 Selecting a proper model	6
2.4 How Geant4 works	6
2.5 Geant4 programming.....	7
2.6 Detector construction.....	7
2.7 The material definition	8
2.8 Physics lists in Geant4.....	9
2.9 Primary generator action	10
2.10 Geant4 models and processes	11
2.10.1 Binary Light Ion Cascade.....	12
2.11 JQMD	13
2.12 G4 Wilson Abrasion Model	13
2.13 Run in Geant4.....	14
3.PARTICLE INTERACTIONS AND ENERGY LOSS IN MATTER.....	15

3.1 Energy loss in matter	15
3.1.1 Particle range calculation	19
3.2 The Bethe – Bloch Formula.....	19
3.3 Electron (positron) interactions with matter	21
3.4 Interactions of Photon with Matter	21
3.5 Photoelectric Effect	22
3.6 Compton effect	23
4.RADIATION THERAPY FOR CANCER TREATMENT	25
4.1 Proton therapy.....	26
4.1.1 Proton range in hadron therapy	26
4.1.2 Types of proton therapy	28
4.2 Laser Therapy	30
4.3 Electron therapy.....	31
4.3.1 Disadvantageous of electron therapy	32
4.4.1 Advantageous of ion therapy to proton therapy	34
4.5 RBE	35
4.6 Carbon ion therapy benefits.....	36
5.ANALYSIS	38
5.1 Fragmentation.....	38
5.2 Charge changing cross section	39
5.3 Simulation of ^{12}C interactions	40
6.CONCLUSION	47
REFERENCE.....	48

LIST OF FIGURES

FIGURES

Figure 2.1: schematic diagram of Geant4 process.	6
Figure 2.2 : ^{12}C fragmentations shown by Geant4 visualization driver.	9
Figure 2.4 : Schematic view of particle gun which accelerates the particle beams toward the detector.....	11
Figure 2.3 : Inelastic collision including abrasion and ablation process in Wilson model.	14
Figure 3.1 : Gaussian surface in coulomb interaction.....	16
Figure 3.2 : Schematic view of photoelectric effect.	23
Figure 4.1 : The relative dose-depth estimations.....	27
Figure 4.2 : Beam deposit energy is transferred to the tumor area.	28
Figure 4.3 : Focusing the beam in tumor volume.	30
Figure 4.4 : A schematics view of laser therapy.	31
Figure 4.5 : A carbon interaction in nuclear emulsion.....	33
Figure 4.6 : A schematic view of proton therapy.....	35
Figure 4.7 : The relative Biological Effectiveness with respect to Linear Energy Transfer.....	37
Figure 5.1: Fragmentation process.....	39
Figure 5.2 : Sample of detector module filled with Lexan layers.	40
Figure 5.3 : A view of ^{12}C interactions in the detector.	41
Figure 5.4 : 3D view of the detector simulated with Geant4.	41
Figure 5.5 : A view of carbon track simulated in Geant4.	42
Figure 5.6 : A view of carbon fragmentation in Geant4.	42
Figure 5.7 : A view of carbon fragmentation in Geant4.	43
Figure 5.8 : Charge distribution of the secondary particles.	44
Figure 5.9 : Range distribution for $z=1$ particles produced from carbon fragmentation.	45
Figure 5.10 : Range distribution for $z=2$ particles produced from carbon fragmentation.	45

Figure 5.11 : Track multiplicity distribution of all vertices..... 46

CHAPTER 1

INTRODUCTION

The first observation of a sudden particle energy loss at the end of its range was reported by William Henry Bragg and Richard Daniel Kleeman for alpha particle and is known as the Bragg Peak [1]. After that, in Berkeley National Laboratory, Robert Wilson get some new results that heavier ions, like Neon and Argon have outstanding advantages in cancer therapy usage with respect to the standard particles, like proton. Heavy ions like carbon shows the discrete characteristics of the Bragg Peak as the dose raises along with the penetration depth into the body, terminating in a keen maximum at the last point of the particle range. As the particles become more dense, the probability of their collision with the tumor decreases and the beam does not extend as much as in the case of the lighter particles. This itself causes not only the beam restricted better in circular direction, but also the Bragg Peak itself is sharper compared with protons range. On the other hand, heavy ions have great capabilities with respect to photons due to better depth dose distribution. Bragg Peak position can be chosen easily in the way that coincides with tumor region, this means that healthy tissues are not damaged. This characteristics guides to still more prominent accuracy in curing tumors in sensitive regions of the body which is hard and risky to do any surgery there [1].

1.1 Clinical application of carbon ions and carbon therapy methods

Maybe one of the remarkable characteristics of the carbon ions is their strongly energy loss or linear energy transfer (LET) system which leads to Bragg Peak creation. Because of their mass, ions need more energy to reach to deeper areas of the medium compared to protons, so in the same depth, carbon ion would have the better energy profile on the tumor which is applicable for the bones, soft tissue arcomas, lung cancer and prostate cancer. In order to accelerate the ions to these huge levels of energy, synchrotrons are better to use rather than cyclotrons which are more useful for the proton acceleration affairs. On the other hand, in order to get a meaningful bending radius in ion therapy, much stronger magnet would be needed which is used in quadrupole magnets of the synchrotrons. This approach leads to giant machines for operating in carbon therapy [2]. However, in radio therapy with carbon ions, we would face with the redundant fragmentation dose beyond the Bragg Peak which can damage the healthy cells. The carbon ion therapy has been favoured rather than other hadronic methods because of its high efficiency [2].

1.2 Radiation therapy and carbon ion therapy advantageous

Before applying the carbon ions in most of the operations, there were many radiation therapy methods like X-ray, using photons in cancer therapy and proton therapy. Some of them are still used depending on condition of the patient.

The history of using photons in medical applications started at the end of the 19th century. The world was excited about the new rays, the X-rays, discovered by Rontgen 1895. Soon the x-rays were used for both imaging and treatment of malign tissue. Since then, the photon therapy has become more and more sophisticated in order to increase the dose given to the tumors and reduce the dose for the normal tissue. Because of the statistical nature of the photon interactions, a beam of many photons is exponentially attenuated yielding an exponential decrease of the dose with

the depth. To obtain a higher dose in the tumor than in the surrounding normal tissue, many irradiation fields are used. The cost of this method is that a large volume of the normal tissue will suffer from a high dose. By replacing the x-rays with high energy photons, the dose maximum is shifted a few centimeters deeper and the exponential decrease is more shallow, which improves the ratio between dose in the tumors and in the normal tissue. With newer irradiation techniques, such as Intensity-Modulated RadioTherapy, IMRT, an improved dose distribution can be delivered. In IMRT, the intensity is not longer constant in each field, but adapted for the geometry of the tumor. Often, the dose given to the tumor can be increased compared to the conventional therapy. With a computer supported planning an optimal treatment plan is obtained where radiosensitive tissue can be spared [3]. Radiation therapy with ions has become an interesting and evolving complement to photon therapy. The reason is that charged particles and photons interact with the tissue in a different way, which leads to a completely different depth dose profile. In contrast to photons, the depth dose profile of charged particles is relatively flat in the entrance channel and towards the end of their range a dose maximum is reached followed by a steep decrease to almost zero dose [3].

This thesis is organized as follows; in Chapter 2 a detailed explanation about Geant4 software is given. Then a brief view to the particle interactions and energy loss in matter are given in Chapter 3. After accomplishing this step, there is an overview to the radiation therapy methods and its classifications in Chapter 4. Real data and Monte Carlo comparisons on fragmentation models have been presented in Chapter 5 and Chapter 6 is about conclusion.

CHAPTER 2

GEANT4 TOOLKIT FOR MONTE CARLO SIMULATIONS

Geant4 in its basic definitions is powerful tool for detector designing and tracking of different kind of particles. Simply one can simulate the passage of the particle through the matter. Geant4 is a assistant toolkit that prepares programmable environment in C++ and supports the object-oriented programming methods (OOP). Covering the different data fields and model of interactions give the Geant4 a reasonable ability to support most of the user needs.

2.1 Software facilities

Nowadays, GEANT has turned to be an effective simulation tool in hadron therapy studies. Detector construction, comprehensive programming language usage and advanced data acquisition capabilities, has introduced this software as one of the powerful facilities in hadronic and high energy physics. In present research, we tried to simulate the carbon fragmentation by using different types of fragmentation models and detectors. As we will see in next chapters, carbon ion is going to be fragmented while interacting with the nucleons of the detector structure. The result of these interactions would be the ions with low charges respect to primary ions. Depending on the direction of the primary tracks and vertex energy of the beams, if the threshold energy or the minimum energy of secondary ions has been satisfied, they can be created after collisions. In hadron therapy, controlling the dose of these secondary ions is the top priority. Just like carbon ions, these secondary particles bear their own Bragg Peaks, which are happen in different depths in body.

Identifying and controlling the secondary ions dose is very important to preserving the healthy tissues from unwanted radiations.

2.2 Geant4 kernel

We highlight few remarkable features of Geant4 in the following items [3]:

- Using low quantity of details which boosts the CPU speed and decreases the simulation time.
- Free installing and updating ability.
- Creating the visualization facilities to witness the events step by step in 3D orientation.
- Data acquisition capabilities with high resolution answers.
- Ability of easy interfacing with other histogramming softwares like root and AIDA.

By the way, Geant4 kernel provides a device to handle these parameters:

- Detector geometry.
- Detector response to different kind of events.
- High resolution data acquisition jobs which is done step by step for each track.
- Controlling the details and types of simulation by defining new methods for each code.
- Stacking and filtering the unwanted events and create proper shortcuts between run manager and stepping action parts.

2.3 Selecting a proper model

To create applicable integration between Monte Carlo simulation and real data, depending on type of experiment and the parameters which are going to be measured, we have to choose a model. However one of our major attempts is finding a model which shows the best agreement with the real data [4].

2.4 How Geant4 works

In principle, this engine is based on stepping manager and physical process which feed the upper layers like tracks. The schematic diagram of a process in Geant4 is shown below:

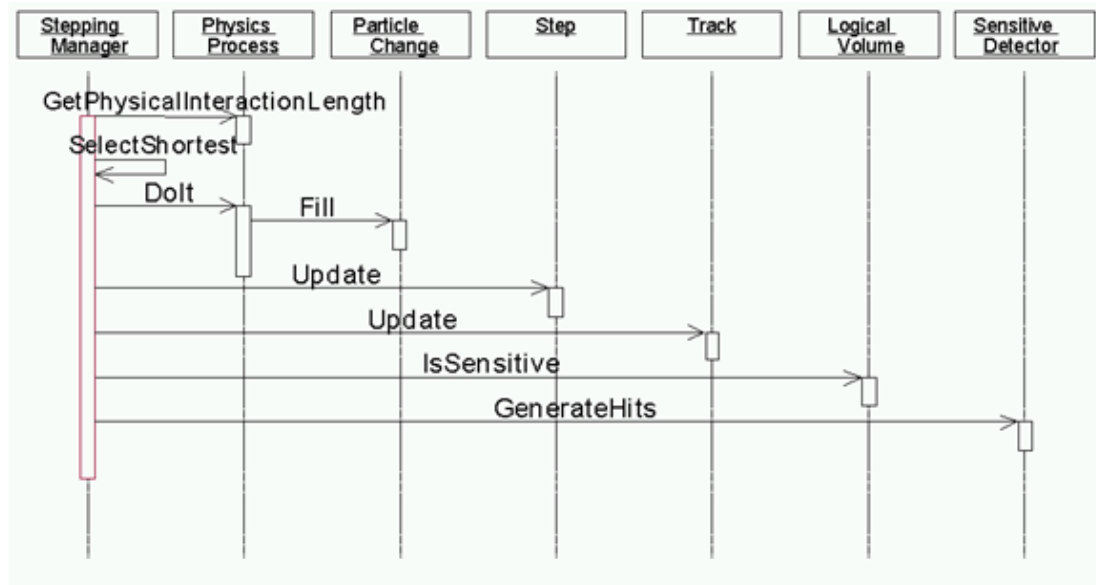


Figure 2.1: schematic diagram of Geant4 process.

In fact, every tracking process is originated from combination of steps. In each step, different characteristics of tracks such as energy, momentum, direction, particle code

and so on can be returned. After each running, these parameters can be accumulated for each track.

Geant4 has a genus structure which has made it unique between other rivals. For example, during an event, when the track is going to be killed or ignored in the detector, the stepping action part of program decides to reset to first step for the new daughter tracks. The similar procedure is performed for every process at the end of each event [5].

2.5 Geant4 programming

We have three models of codes in Geant4 classifications which includes novice, extended and advanced type. Depending on domains of project, one can work with desired category. The advanced codes are more focused on realistic applications of Geant4. These kinds of codes have been gathered by professional working teams of experts. Hadrontherapy, gamma ray telescope and radio protection are the most used classes of advanced codes.

2.6 Detector construction

One of the primary steps in Geant4 is designing and developing the geometry of the detector which is going to be considered as a target for traversed particles. The geant4 presents the facilities in order to handle the geometry of the detector. We can assume this part as physical layout of the detector which is going to be simulated. This layout is playing the role of displaying the behavior of the accelerated particles while passing through the detector. In otherword detector records the effects of these track passings as detector response.

The detector construction source file is a suitable environment which includes the detector construction class for designing the geometry. Principally detector construction is a virtual class which gives the ability of defining the materials, sizes and position of each part of detector. Practically every programmer should consider some steps in coding the geometry definition. The first step is defining a solid volume, which for example can be a cylinder, sphere or cone. The second step is applying a logic volume by adding an electromagnetic field around the detector or adding parameters like color for a better visualization of the target. Finally a physical volume should be defined and the position of different parts of the detector with respect to each other [6].

2.7 The material definition

In the nature, materials are mixture of element and the elements are made up of isotope. In Geant4 the materials are categorized as [8]:

- Isotopes
- Elements
- Compounds and molecules

Based on each classification we have predefined classes in Geant4 as G4Isotope and G4Element. G4Material that covers the physical properties of the matter (pressure, temperature, density, state)

So we can define the preferred elements of our physical volume and sequentially define the materials which are the compounds of these elements [8].

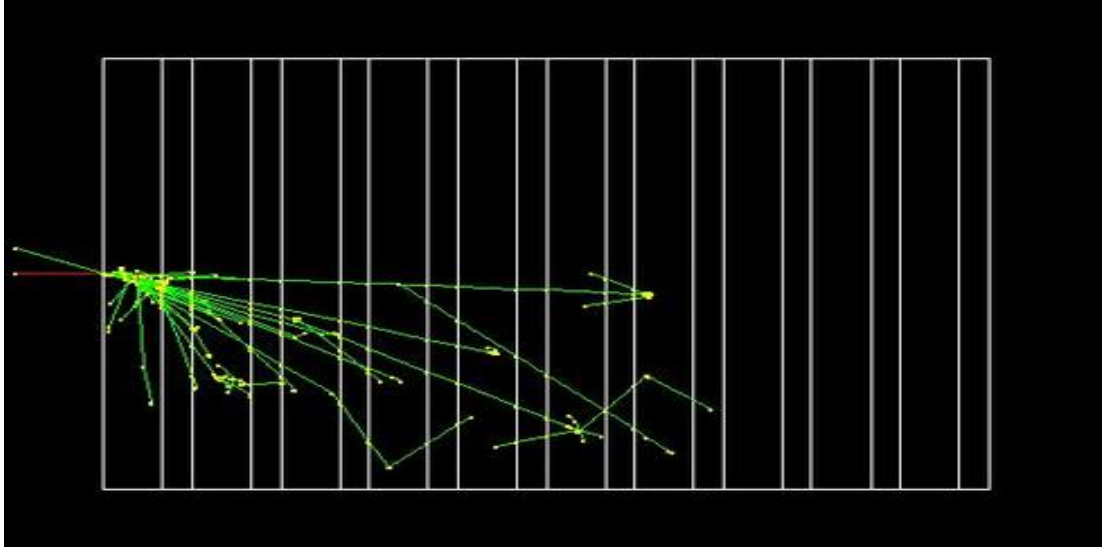


Figure 2.2 : ^{12}C fragmentations shown by Geant4 visualization driver.

2.8 Physics lists in Geant4

In the development of Geant4 we have a lot of predefined physics lists. Here are two available physics lists for hadronic process which has been compared to the experimental data [10]:

- QGSP_BIC
- FTFP_BERT

The other forms of physical lists are manually adapted according to physics process. In these physics list operator has to register the header file of physics list in main code and point to different classes and model available in Geant4. We may have defined different objects inside our physics list, and register our models and process in each category. Here we give most popular types [10]:

- ConstructEM()
- ConstructDecay()
- ConstructHadronic()

As it appears by their name, Geant4 will construct the electromagnetic events in EM and hadronic events in Hadronic classification. In our project, hadronic event are in first priority comparing with EM, since fragmentation of the ions inside the detector is related to hadronic process. Besides that, most of the hadronic modeling such as inelastic and elastic models have to be registered in the hadronic classification. In physics list, there is the capability of setting cuts for each event, in which one can assign the threshold of the secondary productions. This means that in each step, if a secondary particle cannot pass the required threshold it would not be detected. But the important point is, in Geant4 energy steps are equal to range steps inside the detector, so sometimes we can replace them with each other. For example in crossing 1mm distance inside the detector particle may lose the specified amount of energy. We often choose the 1mm or 0.7mm range as a cut off energy [10].

2.9 Primary generator action

Another file which controls the beam definition is the primary generator action. This file contains different kinds of classes such as G4VPrimaryGenerator, G4ParticleGun, G4PrimaryParticle and G4PrimaryVertex. These classes have various types of roles in the primary particle acceleration such as defining the type of particle and controlling its energy and position. By the means of these classes, one has the capability of assigning the primary momentum, initial polarization and vertex position of accelerated particle. The primary vertex position and the slope of primary particles can easily handled in this file. Beside, one can ask Geant4 to accelerate the particles in any angular distribution.

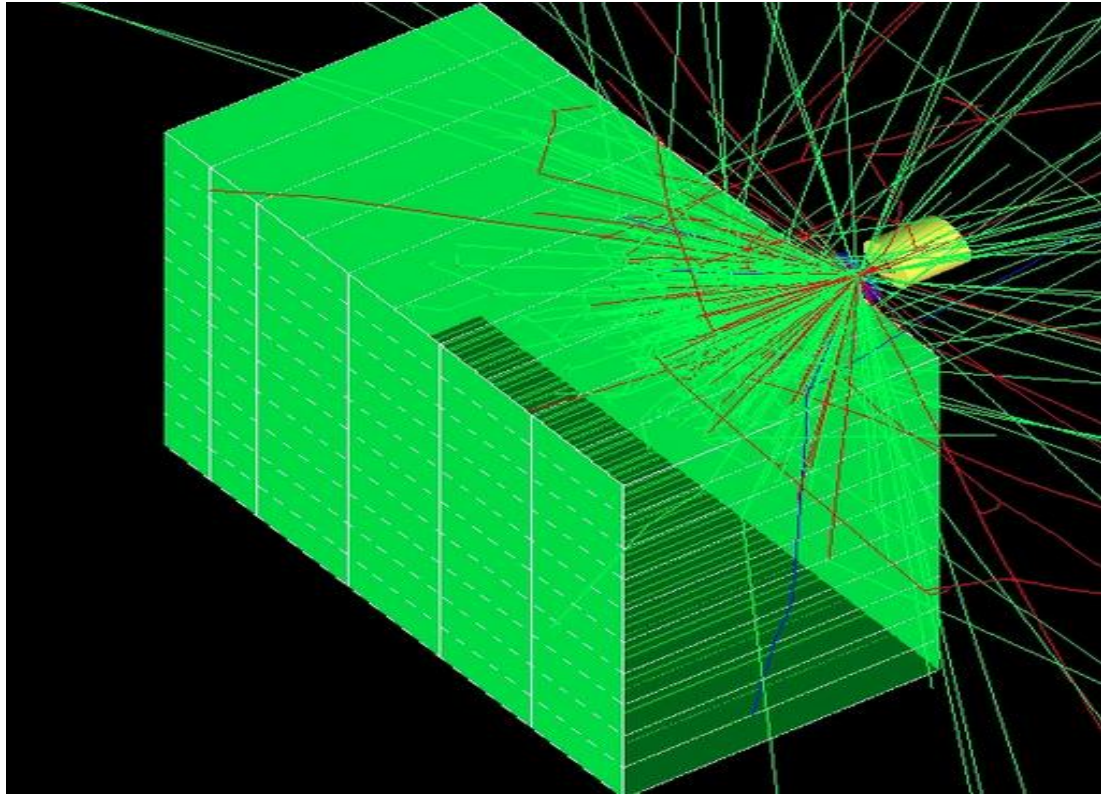


Figure 2.3 : Schematic view of particle gun which accelerates the particle beams toward the detector.

2.10 Geant4 models and processes

Generally we have two types of hadronic models, Low Energy Parameterized (LEP) which is valid for potentials greater than 20 GeV and High Energy Parameterized (HEP) which works for the ionization potentials lower than 20 GeV. Generally process take care of transportation, decays and interactions. Here is number of inelastic models which we have used for Data/MC comparisons [11].

- Binary light ion cascade (extension of binary cascade or BIC models)
- JQMD
- WilsonAblationModel
- BIC (binary cascade)

2.10.1 Binary Light Ion Cascade

Different types of Physics Lists has been provided in Geant4 which are useful according to their specific application domains [12].

The Binary light ion cascade model is extended version of binary cascade model which creates the necessary steps for the hadronic inelastic scattering. This model categorizes the nuclear-nuclear interactions based mostly on geometric argument. In the detector, the target nucleus is assumed as 3D collection of nucleons which is going to be exposed by the accelerated particles. This model intends to explain the propagation behavior of the primary particles [12].

As we pointed before, models work in their special range of energy, this means that if one does not use the proper model for specified interaction, he might lose a part of secondary particles which are not supported by the model energy range, but in fact, they are produced in real experiment. For this model the ionization potential is between 80 MeV/N and 10 GeV/N which supports the wide range of the secondary particles. This model uses the `G4BinaryLightIonReaction` class as a wide range library which is defined for Binary Cascade simulations [12].

`G4BinaryLightIonReaction` is valid for the specific type of particles like [12]:

- Deuteron
- Triton
- He3
- Alpha
- Generic ion

By taking into account that, this model cannot be used for generic ions with atomic number greater than 12.

2.11 JQMD

The Jaeri Quantum Molecular Dynamics (JQMD) is one of the best models to simulate the different aspects of heavy ion reactions. Shortly, the JQMD model can be explained as quantum expansion of the classical molecular dynamics model. The JQMD model is used to evaluate different properties of the heavy ion reactions. In the JQMD code, there are two steps; first, the absolute reactions and the second, kinetic generation of excited fragments which are measured in the form of JQMD model. This additional step is measured by Statistical Decay Model called SDM. The ionization potential of the model is between 0 and 10 GeV [13].

2.12 G4 Wilson Abrasion Model

This model is a simplified version of Binary Cascade which is not mostly recommended in calculations because of its weak domain of ion support. One can illustrate this model as a macroscopic model for nuclear-nuclear interactions based largely on geometric arguments. Since the authority of the libraries are more isolated than the extended models, the speed of the simulation has found to be faster comparing to the models like G4BinaryCascade. The ionization potential of the model is between 70 MeV/n and 10.1 GeV/n [14, 15].

In recent years, Geant4 team has developed better versions of Wilson model with acceptable efficiency but still it is incomparable with the high extension models like Binary light ion cascade. Figure 2.3 shows a schematic view of inelastic collision that includes both abrasion and ablation process in Wilson model [15].

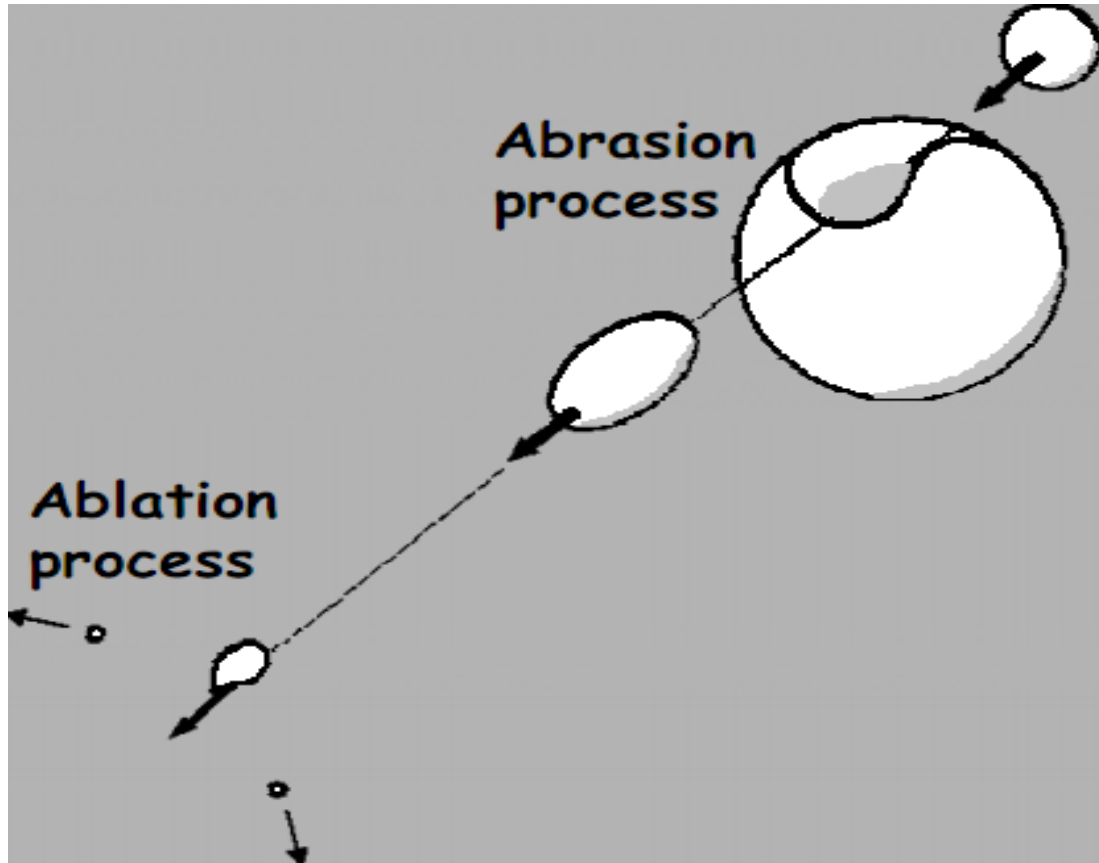


Figure 2.4 : Inelastic collision including abrasion and ablation process in Wilson model.

2.13 Run in Geant4

Before running the Geant4, the geometry of the detector should be optimized and energy cut off values must be defined. After the process we have a list of primary vertices and particles, hit collections. One can easily extract any form of data by creating and opening a text file [5].

CHAPTER 3

PARTICLE INTERACTIONS AND ENERGY LOSS IN MATTER

One of the main parameters that play an important role in particle detection is electromagnetic interactions inside the detector material. In this chapter the main principles of electromagnetic interactions of particles with matter are given.

3.1 Energy loss in matter

Interaction of particles with the matter can be classified as elastic and inelastic interactions. The interaction which results in energy loss and generates excitation of the target atom is the inelastic one. The majority of energy loss is due to electron and ion inelastic collisions. For the first time, Niels Bohr calculated the average energy loss per unit path length yielded from ions inelastic collisions with electrons [3].

In classical view, we can consider the kinetic energy loss of a charged particle in matter due to coulomb interactions. We show a semiclassical argument that demonstrates the energy loss of charged particles in the medium. As shown in Figure 3.1, we consider an incident heavy particle with a specified mass of M and a charge of Z_1e which is accelerated to a speed of v_1 , interacting with the target particle which has the mass of m and charge Z_2e . However we confine to cases where only small momentum transfers occur. This means that the trajectory of the primary particle is not going to be changed significantly and the target particle would have just a little recoil. The moving charge creates an electromagnetic field and since the target

particle is supposed to have only small velocities, the magnetic interaction is not important. By symmetry the net Coulomb force acting on the material particle is perpendicular to the Gaussian surface. The transverse electric field which is produced by the moving charged particle is [28].

$$E = Z_1 e b / r^3 \quad (3.1)$$

where b represents the impact parameter in [28].

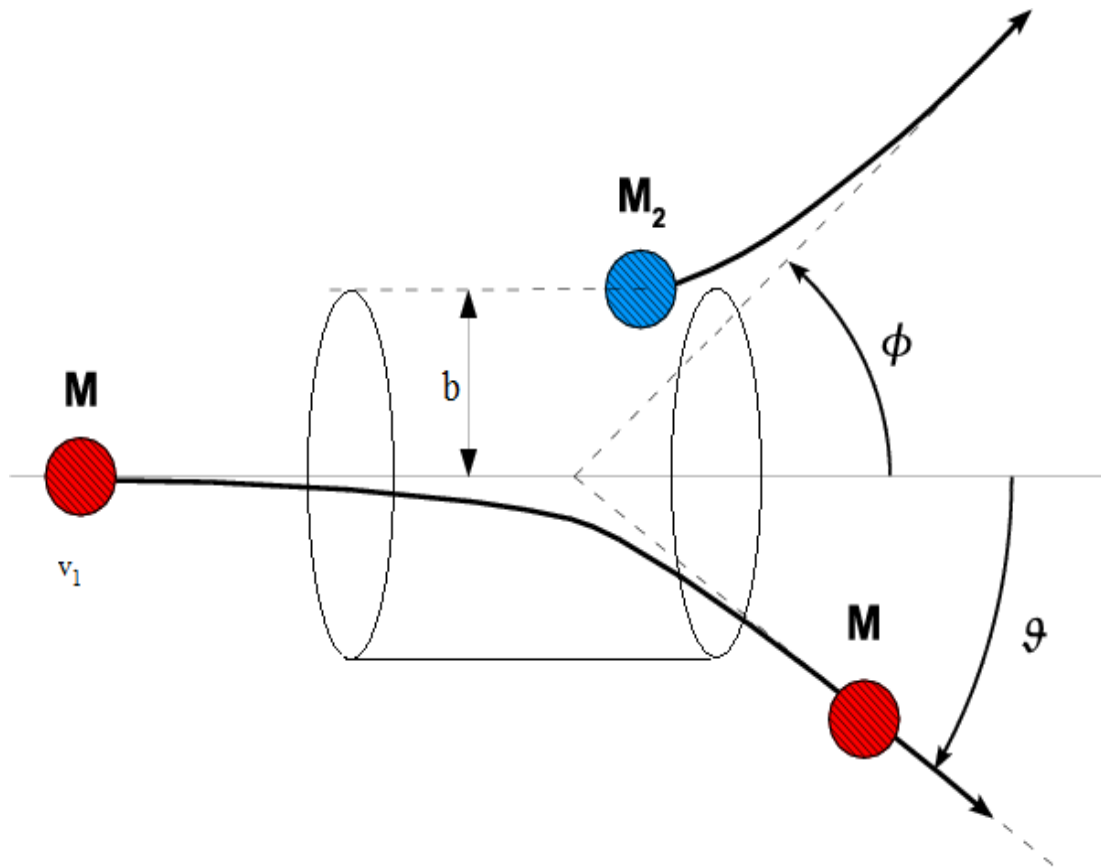


Figure 3.1 : Gaussian surface in coulomb interaction.

The electric field observed in the LAB frame changes with time. Suppose that at time t the transverse electric field in the LAB frame is given by [28]

$$E = \frac{\gamma Z_1 e b}{(b^2 + \gamma^2 v_1^2 t^2)^{3/2}} \quad (3.2)$$

The change on momentum of the incident particle can be written as

$$\Delta p = \int F dt \quad (3.3)$$

$$\Delta p = \int \frac{\gamma Z_1 e b}{(b^2 + \gamma^2 v_1^2 t^2)^{3/2}} (Z_2 e) dt \quad (3.4)$$

$$\Delta p = \frac{2 Z_2 Z_1 e^2}{v_1 b} \quad (3.5)$$

The primary particle will have collisions with both nuclei and the electrons of the atoms. Since the bound particle is assumed to have only a small velocity, the energy transfer can be written as [28]

$$\Delta E = \frac{2 Z_1^2 Z_2^2 e^4}{b^2 v_1^2 m} = \frac{(\Delta p)^2}{2m} \quad (3.6)$$

There are $n_e \times 2\pi b \, dbdx$ electrons in the cylindrical shell shown in the Figure 2.1 where n_e number of electrons per unit volume. So by summing over the total energy transfer in each b interval, the total energy loss per length is

$$\frac{dE}{dx} = 2\pi n_e \left(\frac{2Z_1^2 e^4}{m v_1^2} \right) \int_{b_{\min}}^{b_{\max}} \frac{db}{b} = \frac{4\pi n_e Z_1^2 e^4}{m v_1^2} \ln \frac{b_{\max}}{b_{\min}} \quad (3.7)$$

The limiting values of impact parameter are determined by the range of validity of the various assumptions that made in Eqn.3.7. We have assumed that the interaction takes place between the electric field of the incident particle and a free electron. However the electron is actually bound to an atom. The interaction may be considered to be with a free electron only if the collision time is short compared to the characteristic orbital period of the electrons in the atom, so we have two limits for the impact parameter, where b_{\max} is the upper limit for the impact parameter and b_{\min} is the lower limit for b , and they can written as

$$b_{\max} = \frac{\mathcal{W}_1}{\omega} \quad (3.8)$$

where ω is the characteristic orbital frequency and for b_{\min} one obtain

$$b_{\min} = \frac{Z_1 e^2}{\gamma m v_1^2} \quad (3.9)$$

By substituting the Eqns 2.8 and 2.9 in Eqn.2.7 one can get

$$\frac{dE}{dx} = \frac{4\pi n_e Z_1^2 e^4}{m v_1^2} \ln \frac{m v_1^3 \gamma^2}{Z_1 e^2 \omega} \quad (3.10)$$

We can clearly observe that the energy transfer is inversely proportional to the square of the primary particle velocity and to the square of the impact parameter. This means that the majority of the energy transfer or energy loss is due to the close - collisions where the impact parameter is small [28].

3.1.1 Particle range calculation

One can easily calculate the range of the particle with a kinetic energy of T using Eqn.2.11, in which the particle range or penetration inside the detector is in reverse ratio of energy loss.

$$R = \int_0^T \left(\frac{dE}{dx}\right)^{-1} dE \quad (3.11)$$

3.2 The Bethe – Bloch Formula

Bethe and Bloch performed the correct quantum-mechanical calculation of energy loss in matter. Since momentum transfer is measurable quantity rather than the impact parameter, the calculation of the energy transfer is parameterized in terms of momentum transfer as [3]

$$\frac{dE}{dx} = -4\pi n \frac{Z_T Z_P^2 e^2}{m_e v_P^2} \left(\ln \frac{2m_e v_P^2}{I(1 - \beta_P^2)} - \beta_P^2 \right) \quad (3.12)$$

where,

n : electron density of the target,

Z_T : atomic number of the target

v_P : velocity of the projectile

m_e : the rest mass of the electron

Z_p : atomic number of the projectile

$$\beta = v_p / c$$

I : the mean excitation potential of the target

e : charge of electron

c : speed of light

E : energy of the particle

When the velocity of the projectile reaches to Bohr velocity (electron's speed in Bohr model), the projectile begins picking up electrons, after this step, the nuclear charge, Z_p can be replaced by effective charge Z_{peff} , which is given by [3]

$$Z_{peff} = Z_p (1 - e^{-12.5\beta_p Z_p}) \quad (3.13)$$

Considering the low energy particles, the energy loss increases due to the $1/v_p^2$ dependence. By the way, Z_{peff} gets to zero for decreasing energies. This is the process defined as Bragg Peak phenomenon and has a great importance in the heavy ion therapy. Since the energy loss depends on the square of charge of the projectile, Z_p^2 , the energy loss of carbon ion is approximately 36 times higher than proton of equal velocity [3].

By the way the density effect correction and the shell correction are normally considered in $\frac{dE}{dx}$ estimation. The density correction is important at high energies and but the shell correction becomes more important at low energies. The density effect is due to the fact that the electric field of the particle polarizes the atoms along its path. The shell correction is due to the effects arising from velocity of the incident particle smaller or comparable with the orbital velocity of the binding electrons.

3.3 Electron (positron) interactions with matter

Passing through the matter, electron and positron will have a collisional energy loss like heavy charged particles. Moreover, due to their light mass, electron and positron can do electromagnetic radiation.

In classical case, this kind of radiation is created by the acceleration of electrons and positrons in the field of nucleus. So the energy loss of electrons and positrons can be written as [27]

$$\left(\frac{dE}{dx}\right)_{total} = \left(\frac{dE}{dx}\right)_{radiation} + \left(\frac{dE}{dx}\right)_{collision} \quad (3.14)$$

The basic procedure of collisional energy loss for heavy charged particles can be also used for electrons and positrons but because of their small masses and the collisions of electrons only between the identical particles, the Bette-Bloch formula must be modified [27].

3.4 Interactions of Photon with Matter

The collisional interactions of heavy ions or charged particles shows the small perturbations compared to the light ones. This happens because of the finite energy losses in the beam path. So we would encounter the constant number of particles in a beam and their velocities decrease together. But something different occurs for photons, because there is high probability that an interacting photon will be completely removed from the beam.

The following relation represents the number of photons removed from the incident beam when the photon passes through a material of thickness dx [28].

$$dN = -\mu N dx \quad (3.15)$$

where N is the number of primary photons in the beam and the μ refers to linear attenuation coefficient. In general we can classify the photonic interaction with the matter as follow [28]:

- Photoelectric effect
- Compton effect
- Pair production

3.5 Photoelectric Effect

In this process all energy of the photon is absorbed by an atomic electron. The kinetic energy of the ejected electron is equal to difference of the photon energy and binding energy of the electron. Finally, as shown in Figure 3.2, the electron will move in the perpendicular orientation of primary photon direction [28].

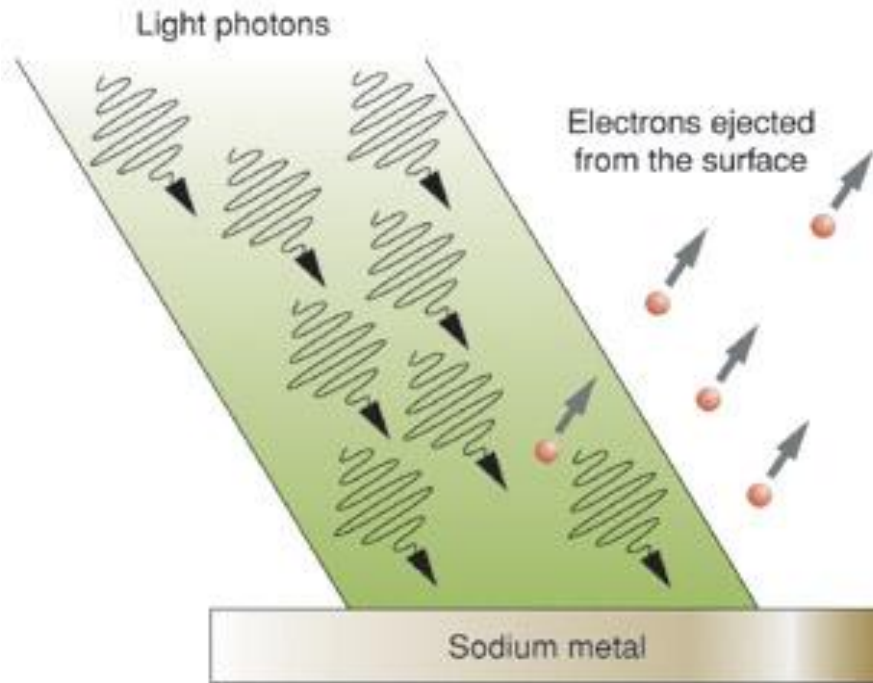


Figure 3.2 : Schematic view of photoelectric effect.

3.6 Compton effect

One can explain the Compton effect as the scattering of an incident photon from an atomic electron. In this interaction, an incident photon with energy of K_0 scatters from an electron which is considered to be at rest. The following relation gives the frequency and the kinetic energy of the recoil electron [28].

$$K_0 + mc^2 = K + T + mc^2 \quad (3.16)$$

$$K_0 = K + pc \quad (3.17)$$

The frequency of the scattered photon is estimated to be [28]

$$\omega = \frac{\omega_0}{1 + \varepsilon(1 - \cos\theta)} \quad (3.18)$$

and the kinetic energy of the target electron is [28]

$$T = mc^2 \frac{\varepsilon^2(1 - \cos\theta)}{1 + \varepsilon(1 - \cos\theta)} \quad (3.19)$$

CHAPTER 4

RADIATION THERAPY FOR CANCER TREATMENT

The main difference between particles and X-ray concerning the cancer therapy is their explicit organic activity and different depth-dose diffusion. For instance in X-rays the dosage declines exponentially as we go more and more deep. So the tumors which are located in deep depths, have to be irradiated in many segmentation in order to protect the healthy tissues around from undesired dose. Beside these approaches, recently high technique of Intensity Modulated radio-therapy (IMRT), which has the capability of exposing up to ten fields from different angles are separately figured and shaped. IMRT yields dominant tumor handling however still a huge volume of healthy tissues may be exposed to radiation. The main trouble of this method in cancer therapy is the orientation and deep position of the tumors.

The compressive clarifications regarding the dose quantity considerations and higher accuracy are possible with particle therapy. Hadron beams have an inverse dose profile that results in a larger dose to the tumor compare with the healthy tissue while entering to the region, however just one treatment is applied. By using developed methods, IMPT, the tumor can be allocated in all its forms with a certainty of near two or three millimeter [16, 17].

4.1 Proton therapy

This method has recently discovered and still requires more research and investigation. The main advantage of proton therapy is that, the radiation dose can be located with a high accuracy [18].

Principally, one can consider proton therapy as a method of external beam radiotherapy which uses ionizing radiation. The accelerated charged particles can damage the DNA of healthy cells too. In fact the cancerous cells are so weak to repair their DNA again, so the dose control of accelerated protons is so important. Figure 4.1 shows a good comparison between relative dose of different radiation therapy methods [18].

4.1.1 Proton range in hadron therapy

Because of their large mass, protons have small oblique side scatter in the tissue; the beam does not expand so much, and this ability helps it to become focused on the tumor region and takes only little dose side effects to the surrounding healthy tissues. All protons with specified energy have a certain range in their path. So few number of protons penetrate beyond that distance. Additionally, the dose which is delivered to the tissue reaches to its maximum quantity at Bragg Peak [19]. Figure 4.2 shows the beam energy focusing, on the tumor region [19].

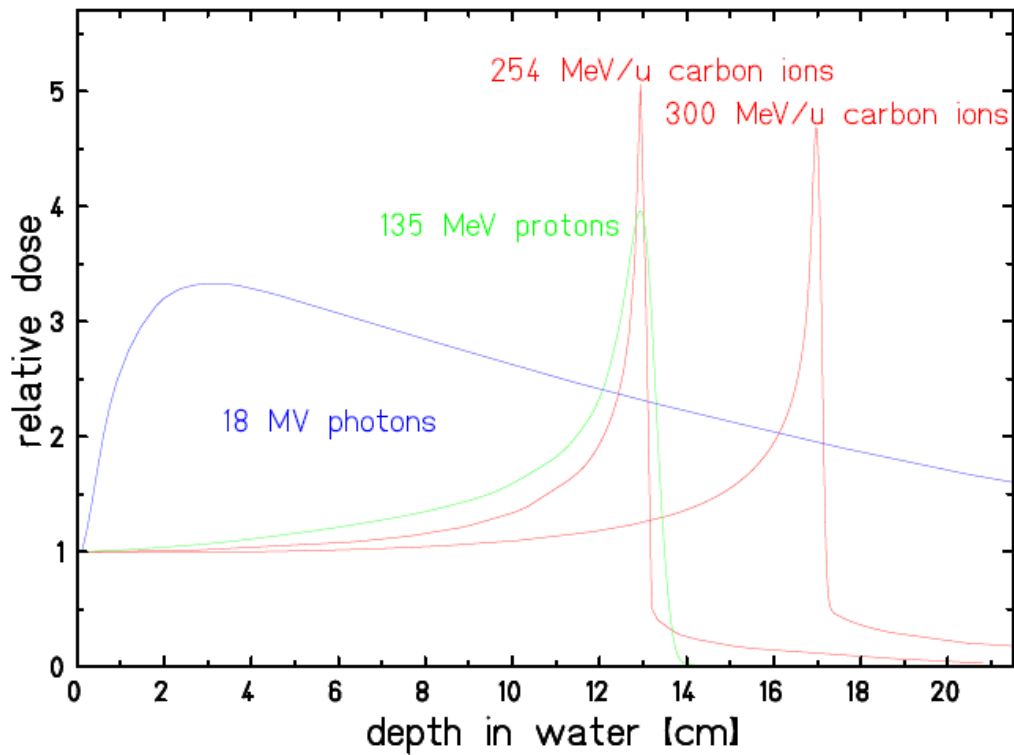


Figure 4.1 : The relative dose-depth estimations.

In order to cure the tumors which have been located in deep in the body, the accelerator must produce a proton beam with wide range of energy. Tumors which are closer to the surface of the body are subjected to low energy protons. Nowadays the accelerators which are used for proton therapy typically produce protons with energies in the range of 70 MeV to 250 MeV. One can increase the cancer cell damage rate, by controlling the energy of the protons during the treatment. As estimated before, the tissues which are closer to the surface of the body receive less radiation energy than tumors, this leads to low damage to healthy tissues. On the other hand the tissues which are located in deeper positions get very few numbers of protons.

The full scale radiation dosage of the protons has been defined as the spread out Bragg Peak (SOBP). It's essential to consider that the deep tissues which are located behind the tumor region will receive no radiation from proton beams [18, 19].

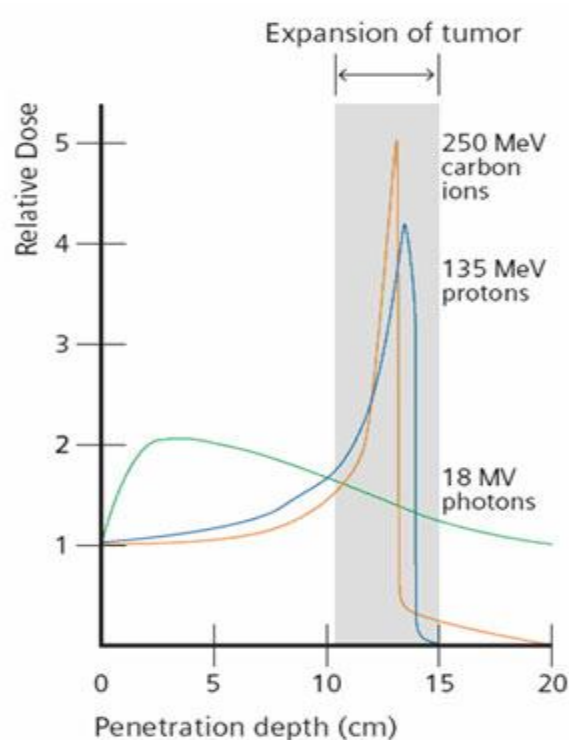


Figure 4.2 : Beam deposit energy is transferred to the tumor area.

4.1.2 Types of proton therapy

The types of tumor therapy in which protons are used can be classified into two categories. As primary we can refer to those for disease sites that acquire the higher doses of radiation, for example dose escalation. In some types, dose escalation is applied and by this way one can increase the quality of curing. These include unresectable sarcomas [19]. The second class includes those treatments where the increased accuracy of proton therapy is utilized to reduce undesired side effects. In these types the tumor dose is the same as that used in typical therapy, and thus there is no assumption of a high probability of curing the disease. Alternately, the priority is on the reduction of the integral dose to normal tissue, and so this causes a reduction of undesired effects. As two remarkable cases we can state pediatric neoplasm like medulloblastoma and prostate cancer [19].

Proton beam behaviors in the matter, has caused a decreasing effect in long term rectal damaging when the treating method is by the means of protons rather than photons, X-ray or gamma ray therapy. The results in other experiments have showed the difference is so small, and is just confined to conditions where the prostate is almost entirely close to special anatomical structures. The relatively trivial progress found may be the result of incompatible patient set up and enclosed organ displacement during treatment [19].

The proton treatment methods used for ocular tumors is an appropriate case since this treatment needs a relatively low energy which is about 70 MeV. Being bounded to this minimal energy ranges, some hadron therapy centers in the world only treat ocular and eye tumors. Position confirmation and modification have to certify that perceptive tissue like the optical nerve region is kept out from the radiations in order to shelter the patient's vision from harmful effects. Figure 4.3 represents the external schematic view of beam gun filtering mechanism [19].

According to the tumor type, the surgery team decides to use the surgery methods or the hadron therapy. For example in some cases surgery is the best choice prior to other methods, cutaneous melanoma for instance, in some other items radiation is most applied for example skull base chondrosarcoma, and in some instances it's hard to decide they are comparable, the prostate cancer is one of them. However experiences have proved that in some cases they should be used together for example rectal cancer or early stage breast cancer [19]. Figure 4.3 shows the beam energy in case of focusing mechanism, on tumor volume in the patient body [19].

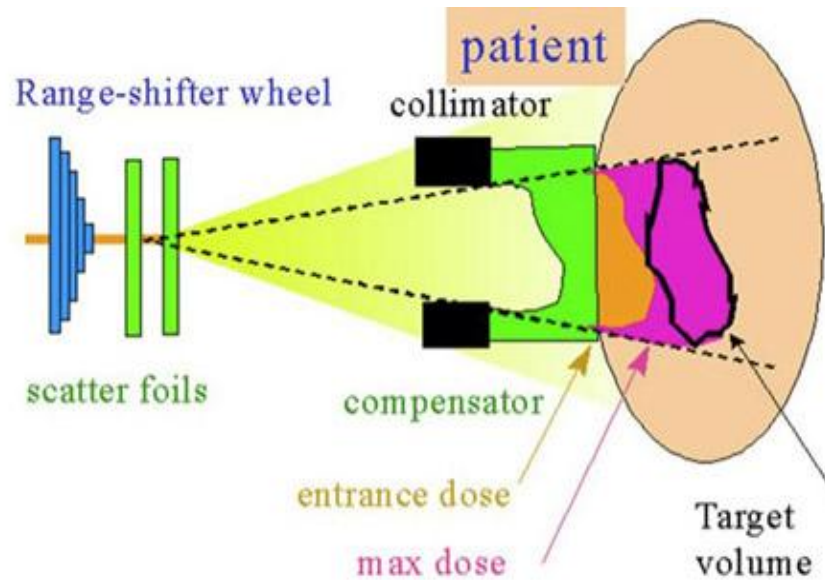


Figure 4.3 : Focusing the beam in tumor volume.

4.2 Laser Therapy

In laser therapy, only small mirrors are needed for laser beam transport unlike heavy magnets in hadron therapy. In other words, the total laser therapy equipment is much inexpensive and lighter than the current hadron therapy machines. One of the other benefits of the Lasers is reduction of the expenses relevant to long shielding tubes which are used in accelerator with tens of meters size far away from the patient. Since hadronic transferring system has to be perfectly radio protected by thick concrete layers the operation costs is so high. In comparison, laser safety is much simpler since it only requires simple systems like plastic screens, fast shutters etc, to prevent from damaging medical staff or patient eyes, but the main problem is the less beam power which is not capable in most of the cases. Figure 4.4 shows the schematics of laser therapy equipment [21].

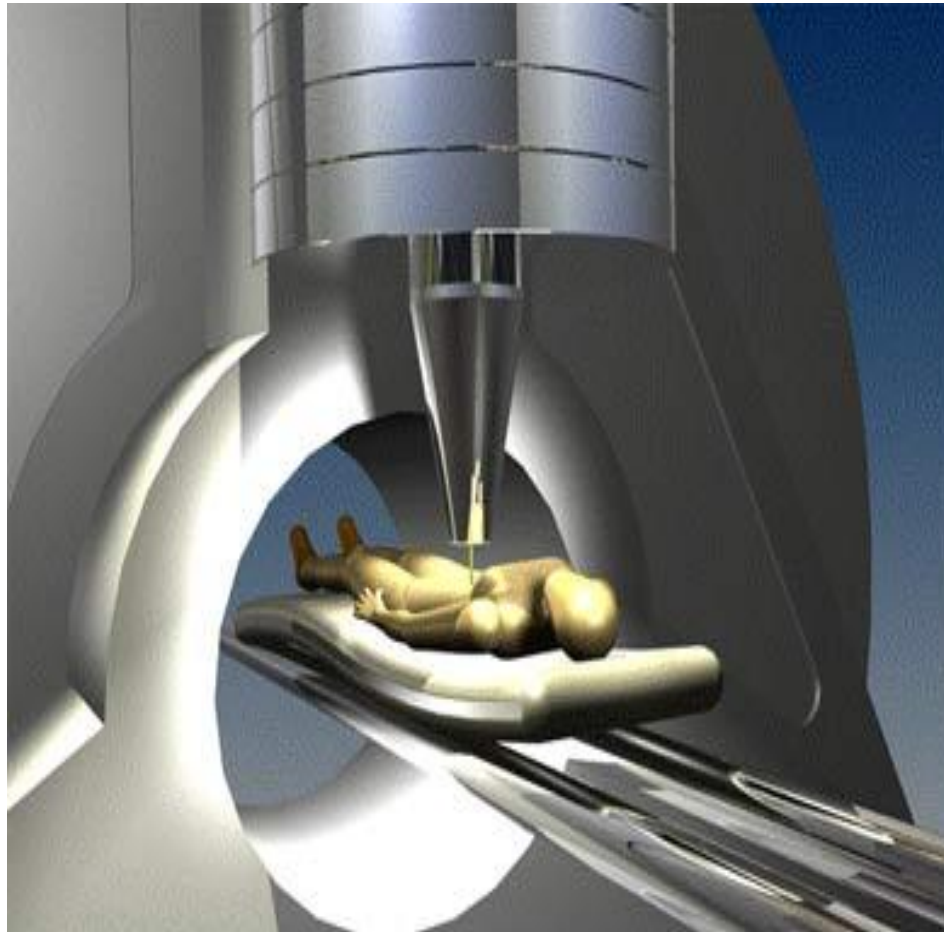


Figure 4.4 : A schematics view of laser therapy.

4.3 Electron therapy

In this method which is called Electron Beam Therapy (EBT) an external current of electrons are directed to the tumor region. This type of cancer therapy is accomplished by using a medical linear accelerator. These machines have the capability of producing electrons up to 20 MeV [22].

4.3.1 Disadvantageous of electron therapy

Unfortunately electron beams lose their energy after crossing a short distance so their range is finite in different areas, so after this effective range their doses diminish rapidly. So they seem to be useless in deep tumors. As other methods in hadron therapy, one can handle and control the beam in desired depth of treatment by managing the energy of the electrons. The light mass of electron leads to low momentum that yields a few numbers of interactions comparing with carbon therapy and even proton therapy methods [23].

4.4 Carbon ion therapy method

Due to its heavy mass, carbon ions can cause on unrecoverable damage to the tumor. However they give a minimum damage to the healthy tissues while passing through the body. By the way, one can control the depth of ion penetration to the patient body easily, and suit the energy deposition near to the tumor. Similar to an explosion inside the tumor when the ions reach to the target zone, they deposit a narrow energy band on the tumor. The treatment becomes challenging and critical job when the tumor area is located near a sensitive organ like eye or brain.

Nowadays, carbon therapy methods are applied for patients in different range of energies like 400 or 300 MeV/n all around the world. Cancer therapy methods using heavy ions, create a high localized energy deposition near the tumor region and current experiments has showed that this method provides a better efficiency with respect to photon and proton therapy. However the secondary particles can cause an unwanted dose beyond the Bragg Peak. It can damage healthy tissues. Therefore, for an accurate dose adjustment, the charge changing cross section has been measured precisely. Estimating the fragmentation of carbon ion is so essential not only for the patient treatments but also for the personnel who are responsible for the operation

due to the radiological risks in space. On the other hand, the fragmentation of carbon ion is not completely discovered yet. Until now, various experiments have conducted using different techniques and detectors in order to measure the primary ion fragmentations. Among all these, nuclear emulsion has distinct properties. Emulsion Cloud Chamber (ECC) which is placed transverse to the beam consists of nuclear emulsion as an active material and lexan as a passive material. This special detector has the ability of space dose distribution analysis. This includes the information like the vertex position, track range and angular distribution of primary and secondary particles [3]. Figure 4.5 shows the carbon fragmentation in ECC.

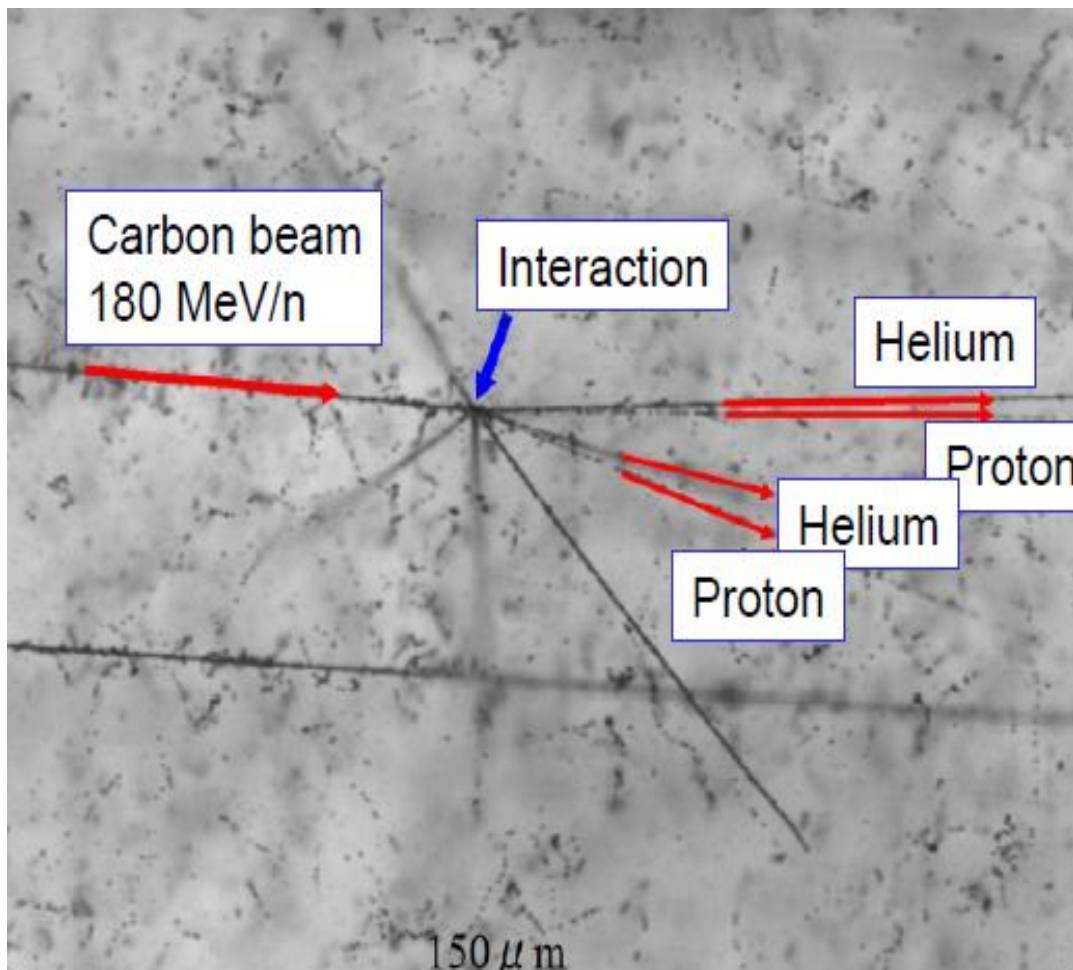


Figure 4.5 : A carbon interaction in nuclear emulsion.

4.4.1 Advantageous of ion therapy to proton therapy

For the carbon ions rather than protons, the sidelong and range is much shorter because of their higher atomic numbers. We can say one of the main benefits of heavy ion tumor therapy is the expansion in relative biological effectiveness (RBE) of particle beams at the end of their range for example in the tumor region. This extended operation has to be considered for treatment intentions. The RBE factor depends on sophisticated parameters and their combination like energy and ion, their dose level, depth in tissue and of course the tissue types itself. When we utilize the ion beams in tumor therapy, if we want to increase the level of RBE, undesired dose should be decrease to the standard amplitude. In principle, because RBE parameter changes with depth, the form and configuration of the depth dose profile has to be adjusted respectively. This method is in order to not let the unwanted dose entering to the healthy profile of the tissue. Mostly, ions are the best substitute for radio resistant tumors; simultaneously protons decrease the hazard of presence of the secondary tumors [20].

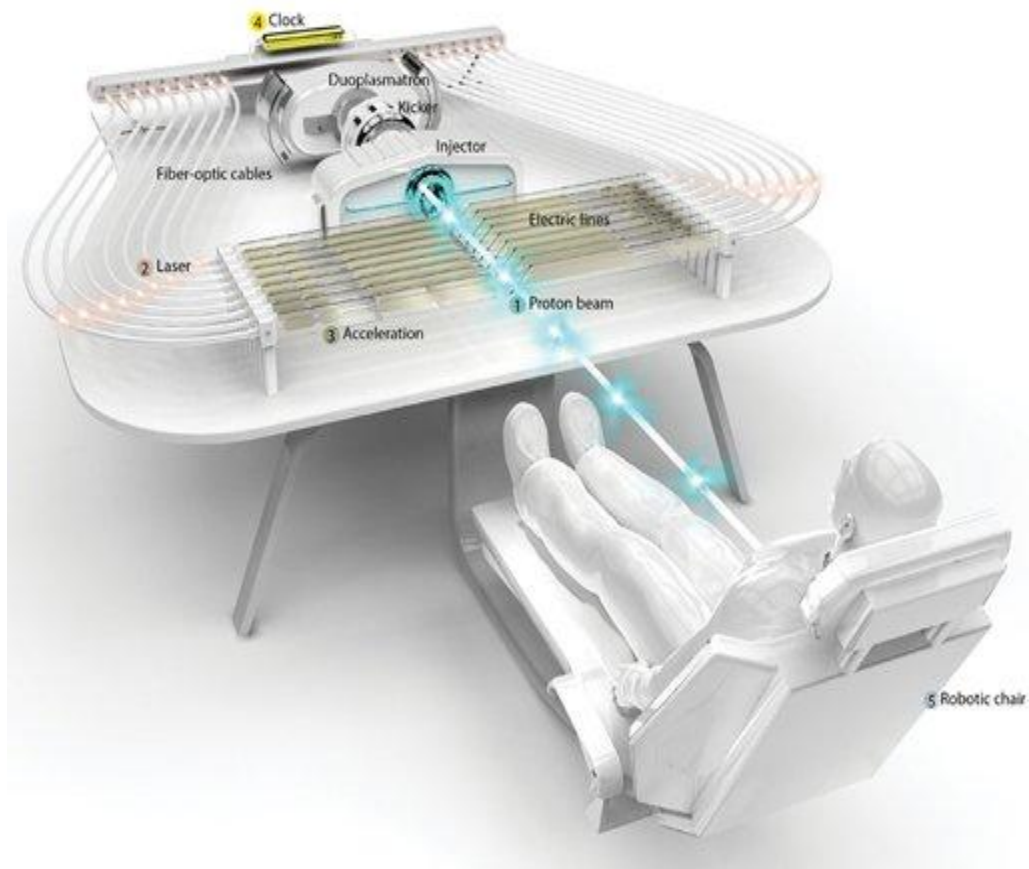


Figure 4.6 : A schematic view of proton therapy.

Figure 4.6 shows a schematic view of proton therapy. Typically, there are two kinds of facilities called eccentric or isocentric machines which are used to carry the proton beams from accelerator to the tumors region. These huge frameworks consist of heavy magnet for beam deflection which weights from 100 to 200 tones and have a diameter from about 4 to 10 meters, accommodated so tightly in a hospital.

4.5 RBE

The range of carbon ions is much shorter compared to the protons due to their higher atomic number. The RBE is defined as the dose of a reference radiation, usually X-

rays, is required in order to have the same biological effect as was seen with a test dose of another radiation. That is

$$\text{RBE} = \frac{\text{Dose from reference radiation}}{\text{Dose from test radiation}} \quad (4.1)$$

In order to increase the level of RBE, the undesired dose should be decreased to the standard amplitude. In principle, since RBE parameter changes with depth, the form and configuration of the dose profile has to be adjusted respectively.

4.6 Carbon ion therapy benefits

Following properties are the main highlights of carbon ion therapy [29]:

- Carbon ions have great characteristics of depositing their maximum energy density at the last steps of their range, called Bragg Peak. This released energy can give a severe damage to tumor.
- Because of collisional characteristics of heavy ions, which has been clarified before, carbon beams can simply be shaped as narrow focused and directed into arbitrary penetrations depths. However the longitudinal and lateral scattering is three times smaller than for protons.
- Carbon beams have a convenient depth profile of RBE. Maybe one of the main priorities of the carbon ions respect to protons, is the low RBE values in beam entrance. Besides that, we can observe significantly RBE increment in the last 2 or 3 centimeter of the range. Figure 4.7 represents the RBE – LET relation for different treatment methods.
- We can arrange the exact location of the carbon ions deposition by the online positron emission tomography called PET. This system allows the beam to be

focused in millimeter precision on the tumor area. This means that the sensitive organic parts such as optical nerve which are located near to tumor can be preserved from damage.

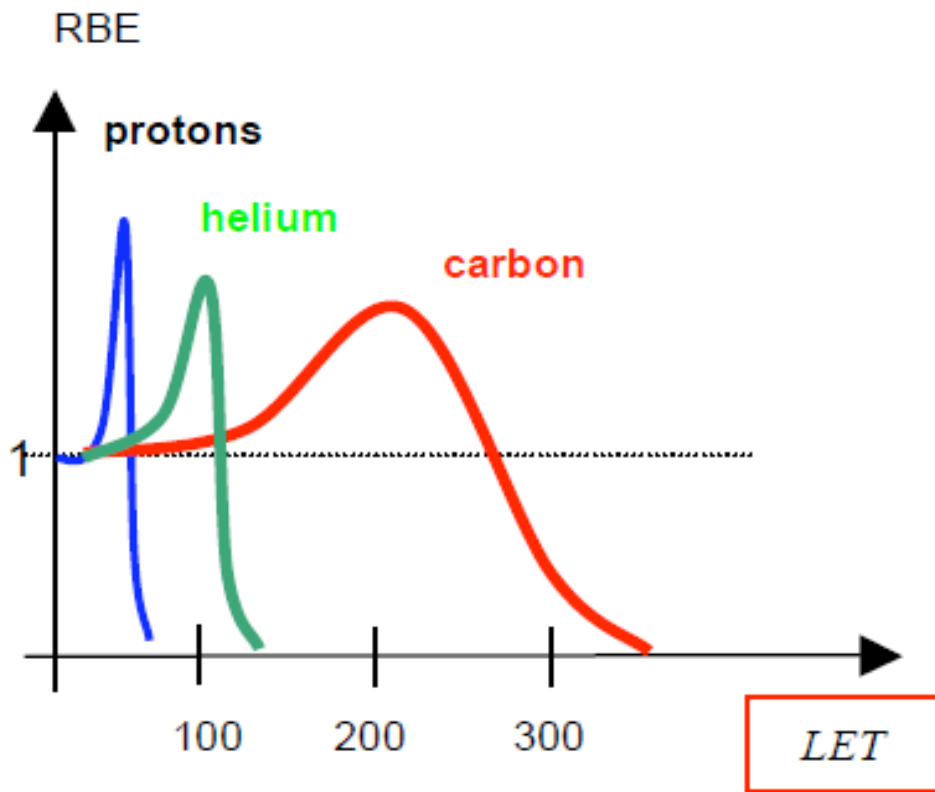


Figure 4.7 : The relative Biological Effectiveness with respect to Linear Energy Transfer.

CHAPTER 5

ANALYSIS

In this chapter we present Geant4 based simulation of ^{12}C interactions in the detector which consists of nuclear emulsion films and lexan layers. The simulation is then compared with real data. As discussed in Chapter 3, Geant4 is the most updated and powerful Monte Carlo tool developed at CERN (European Organization for Nuclear Research). This software has been developed for simulating the beam of particles that pass through material like detector medium.

5.1 Fragmentation

In particle penetration process not only the energy of the primary ions are lost but also they can make nuclear interactions and create new particles. One of the models which explain the nucleus-nucleus interaction is known as abrasion-ablation in Wilson model, which is not capable in defining the non ion models like proton and alpha processes. If we define the primary particle and the target, as participants, and the remaining segment of the particle and target as spectators, we can observe that the spectator projectile continues its path without any change in its velocity and direction, while the target spectator comes to the rest. In this process there would be a group of clusters that consist of the light particles like deuterons and tritiums. Note that these particles are undefined in abrasion-ablation model database. Figure 5.1 shows the fragmentation process which occurs in two steps [3].

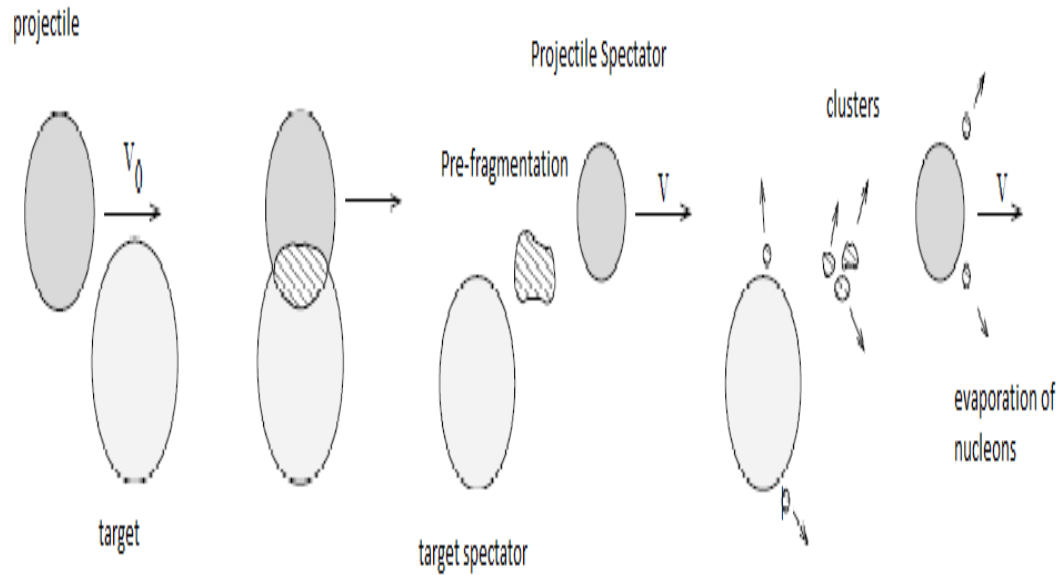


Figure 5.1: Fragmentation process.

5.2 Charge changing cross section

The partial charge changing cross section can be clarified as the cross section of secondary ions production with charge difference $\Delta Z = 6 - Z$. The charge changing which results from carbon interactions are in the range of $\Delta Z = 1, 2,$ and 3 and consist of 21, 23, and 24 % of whole charge changing respectively, similarly this measurements are 16, 33, and 4 % for carbon-polycarbonate interactions. Estimating the charge changing cross sections is an essential step toward the better controlling of the secondary dose profile in cancer therapy [25].

The carbon ion fragmentation has been measured in several experiments using nuclear emulsion [25,26]. As a detector, nuclear emulsion films interleaved with lexan absorbers are used.

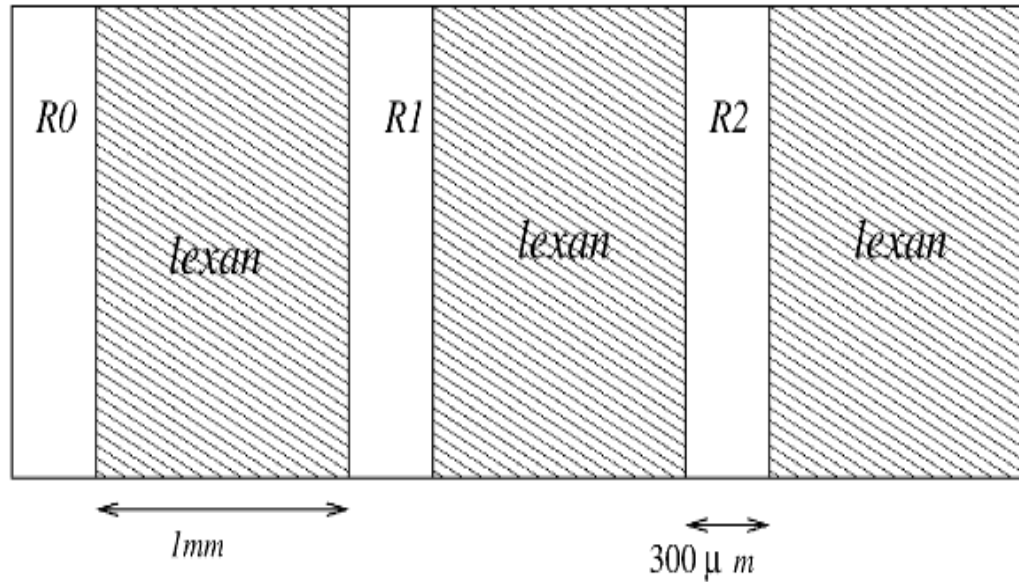


Figure 5.2 : Sample of detector module filled with Lexan layers.

In Figure 5.2, R_0 , R_1 and R_2 are nuclear emulsion films which provide a sub-micron spatial resolution for fragmentation measurement. In other experiment [25] used water instead of lexan layers as a tissue equivalent material. If we compare the electron density of the water $3.3 \times 10^{23} \text{ gr/cm}^3$ with Poly methyl methacrylate (PMMA) target density $3.7 \times 10^{23} \text{ gr/cm}^3$, they have similar properties. So the targets have similar nuclear properties leads to similar interaction ranges [26].

5.3 Simulation of ^{12}C interactions

In order to simulate the ^{12}C fragmentations in an emulsion detector with lexan layers, the slope of ^{12}C ions are set between -0.34 rad and 0.34 rad and they are accelerated to the energy of 400 MeV/n . Figure 6.1 shows simulated detector side view, the red tracks refer to particles with negative charge (here electrons), blue tracks refer to positive charge particles and the green tracks corresponds to the neutral particles.

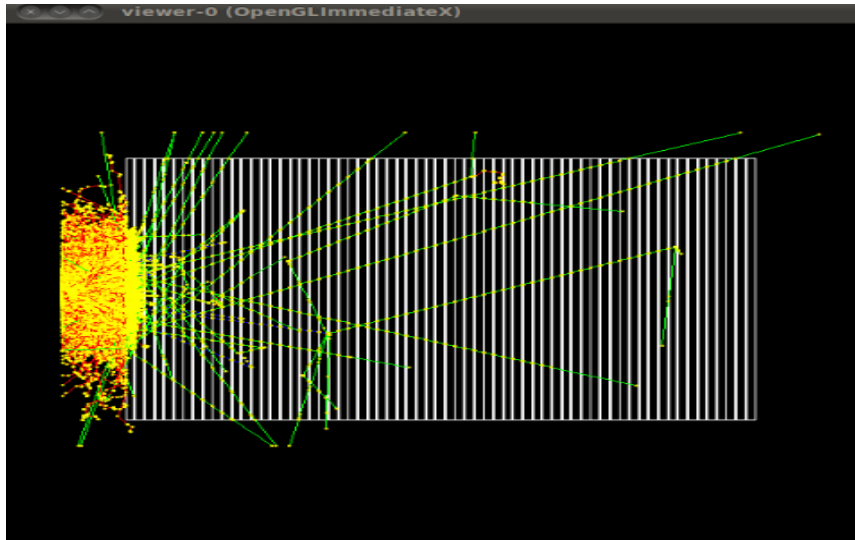


Figure 5.3 : A view of ^{12}C interactions in the detector.

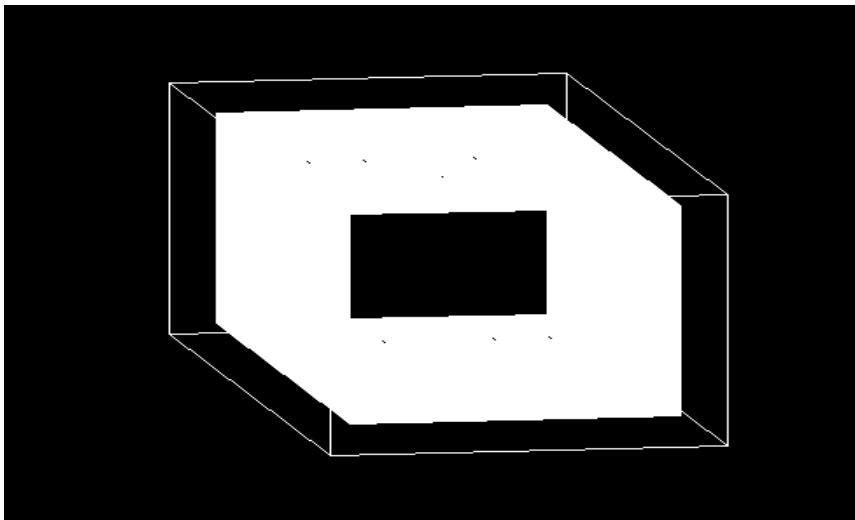


Figure 5.4 : 3D view of the detector simulated with Geant4.

Based on Geant4, about 72% of the incident carbon ions interact before reaching to the Bragg Peak point. Figure 5.5 shows that carbon ion stops without fragmentation.

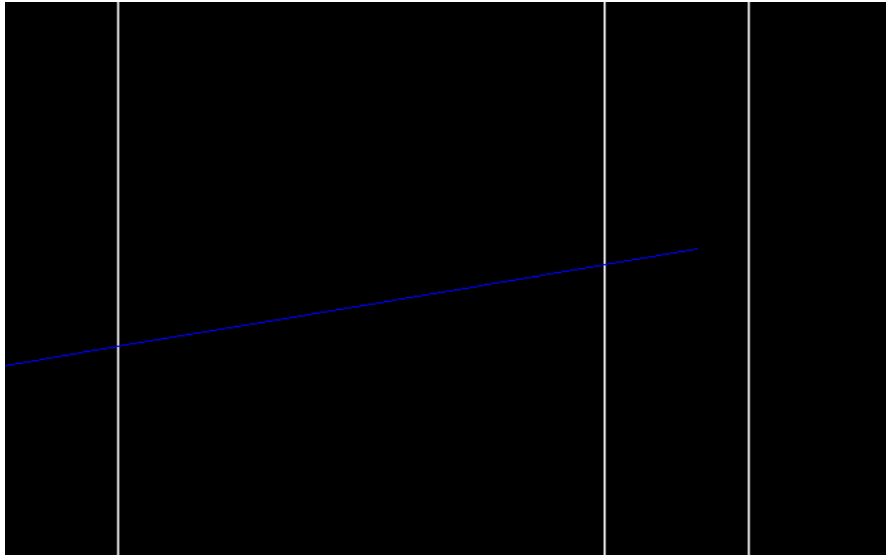


Figure 5.5 : A view of carbon track simulated in Geant4.

As we know, considerable number of carbon ions interact with detector medium and produces the lighter ions, Figures 5.6 and 5.7 show the carbon ion interaction in the lexan layer producing secondary ions.

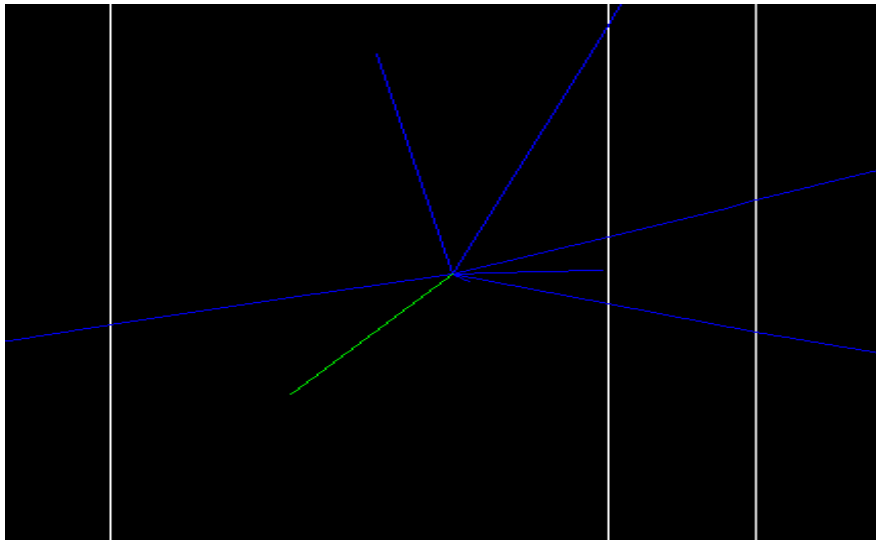


Figure 5.6 : A view of carbon fragmentation in Geant4.

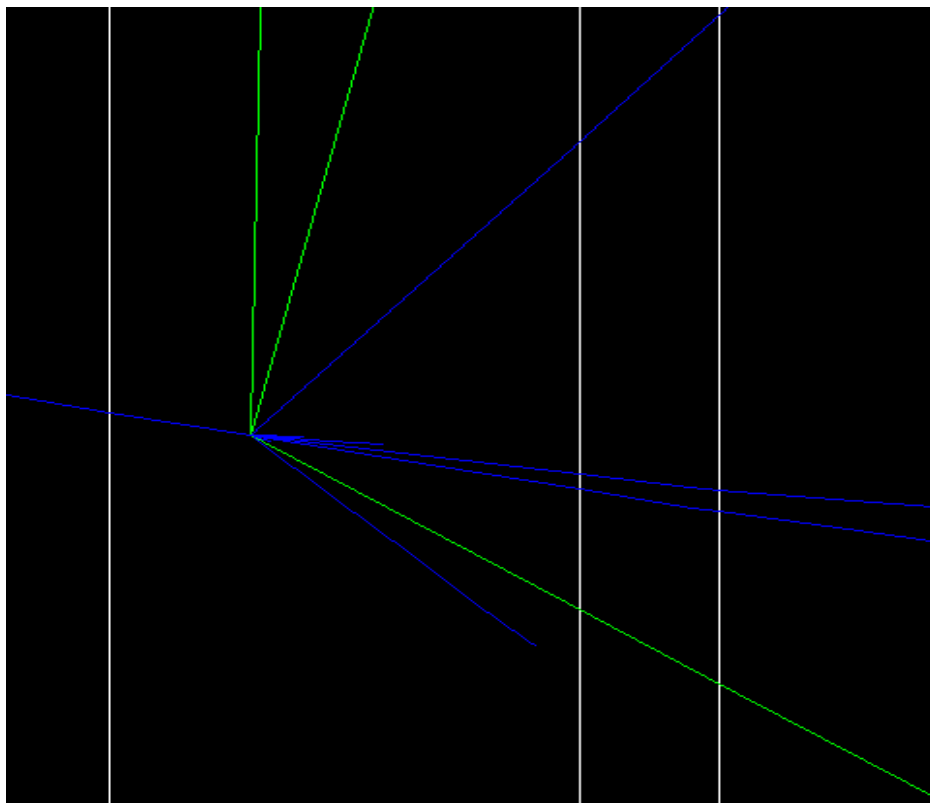


Figure 5.7 : A view of carbon fragmentation in Geant4.

In the following, we are going to compare the real data [26] with Geant4 based simulation. Every particle which deposits its energy and stops inside of the detector can be used for vertexing. However, the track which is created from single prong interaction cannot be distinguished from primary carbon ion if the scattering angle is small. As a result, the analysis of the ionization along the particle track may show a discontinuity at some point which denotes the charge-changing process.

In our simulations, we have used four different models of nuclear interactions for Data/MC comparisons. These are binary cascade [11], JQMD [11], light ion model [11] and the Wilson [11].

Figure 5.8 refers to the charge distribution of the secondary particles which is compared with Monte Carlo results. Concerning the charge distribution, the JQMD model shows a good agreement with real data. Indeed BIC and light ion models show also a reasonable agreement with real data but Wilson model has the largest dispersion.

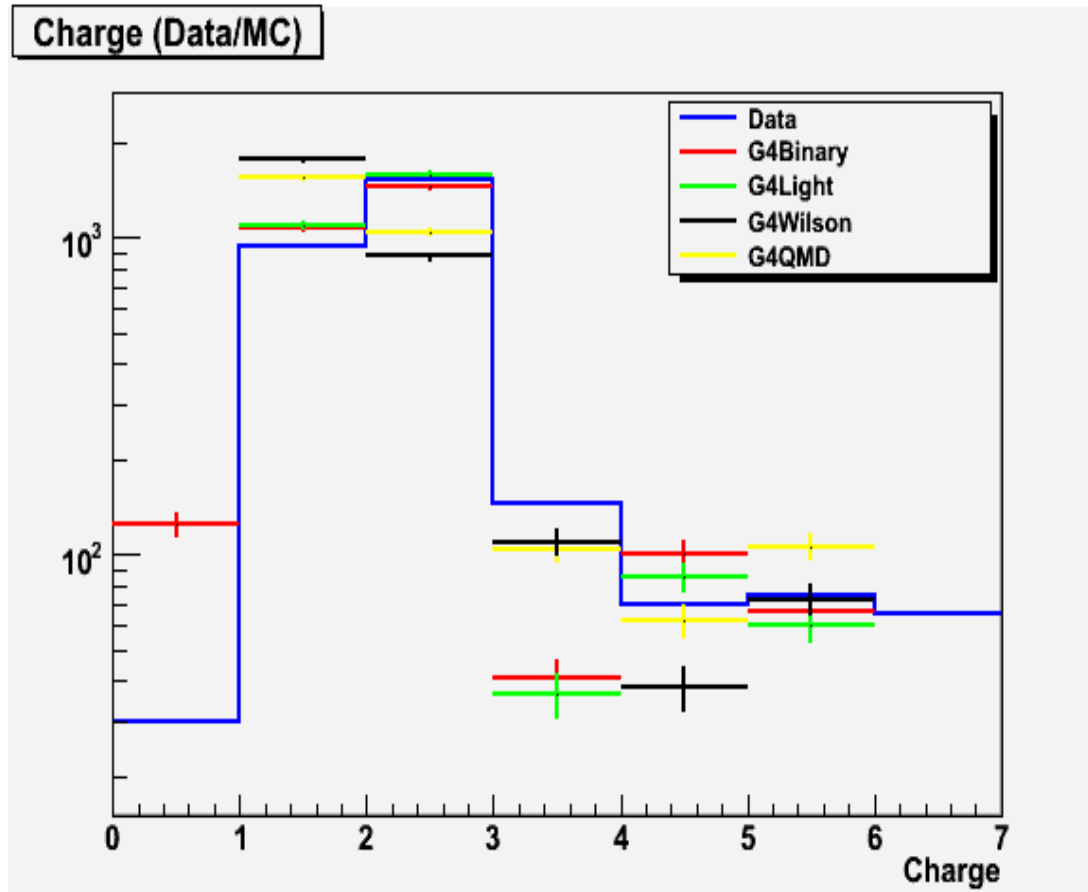


Figure 5.8 : Charge distribution of the secondary particles.

We can say that about 20% of hydrogen ions or protons and 10% of helium ions stop inside the detector volume after depositing their energy. These ions stop before achieving the Bragg Peak. In Figure 5.9 and 5.10 the blue line shows the real range of these ions inside the detector while the other colors refer to the different hadronic models used in GEANT4 [26].

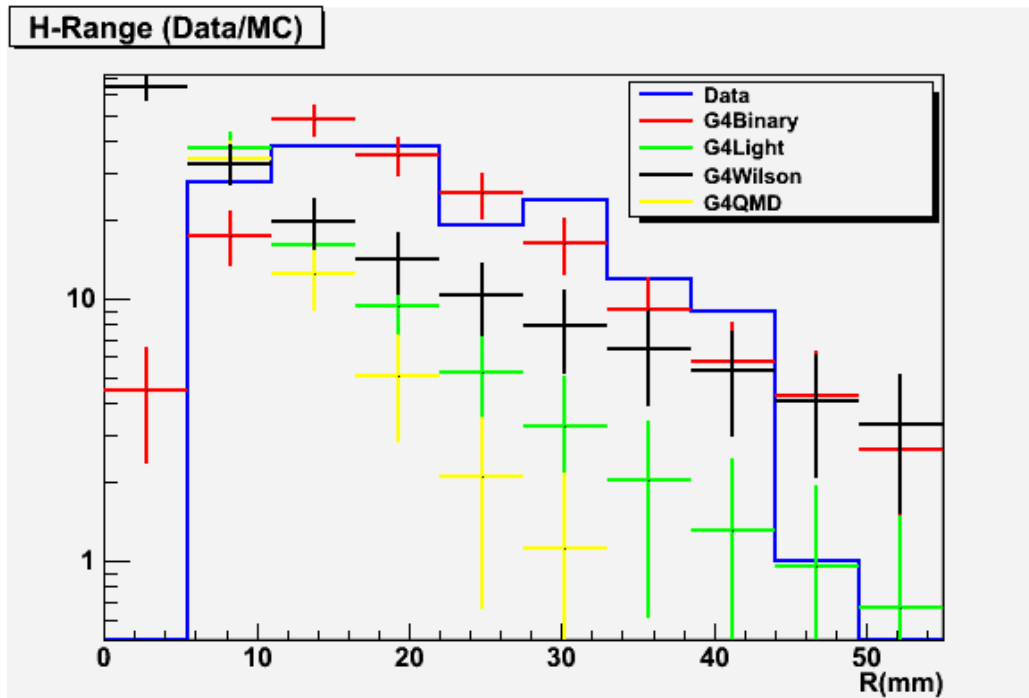


Figure 5.9 : Range distribution for $z=1$ particles produced from carbon fragmentation.

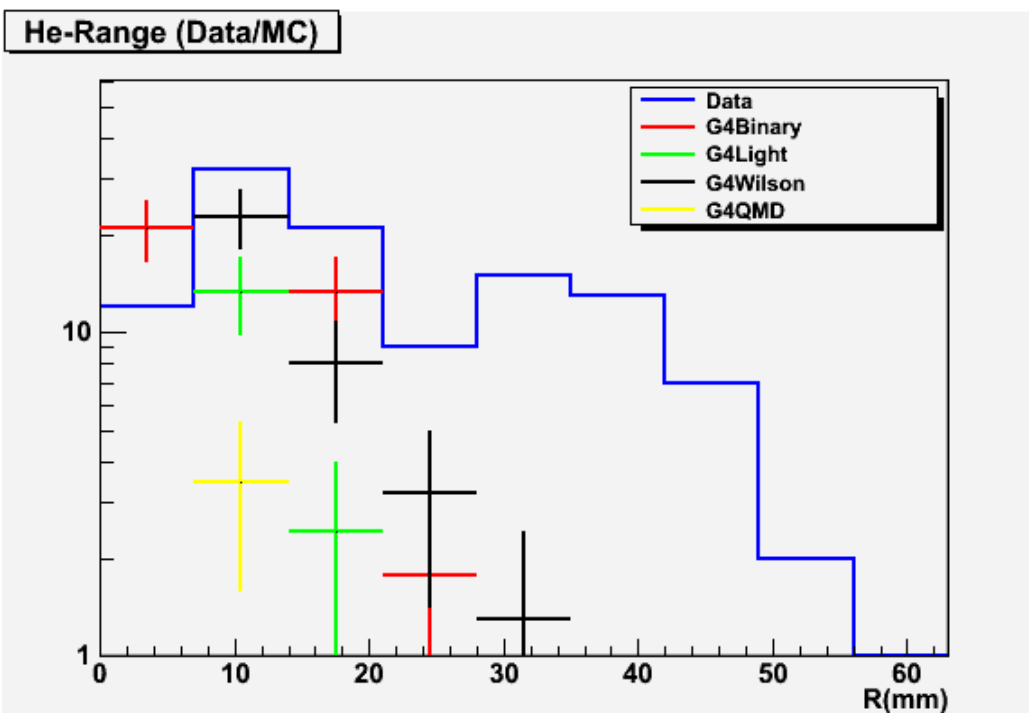


Figure 5.10 : Range distribution for $z=2$ particles produced from carbon fragmentation.

Figure 5.11 shows multiplicity distribution of the real data and Monte Carlo events [26]. Concerning the multiplicity, the data agree with BIC model, it reproduces the data up to multiplicity 5. After multiplicity 5, there is a clear offset, this could be due to cut off values of secondary ions energy.

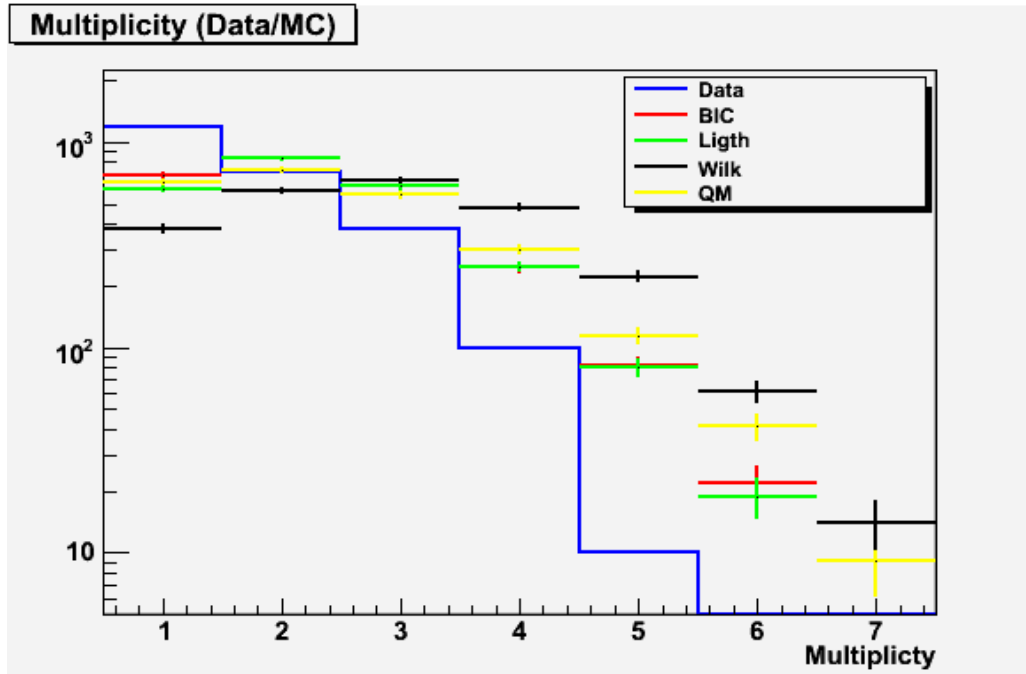


Figure 5.11 : Track multiplicity distribution of all vertices.

CHAPTER 6

CONCLUSION

One of the primary questions that comes to our mind is what is the main advantageous of hadron therapy compared to X-ray and gamma ray therapies. The main advantageous of the hadron therapy is low radiation dose to the surrounding healthy tissues. It is 60% lower than the other methods, depending on the location of the tumor in the body. The main side effect of using X-ray or gamma in cancer therapy is the redundant dose beyond the radiation tumor. This dose can also give damage to the healthy tissues located before or beyond the tumor. On the other hand, carbon ions or protons deposit significant amount of their energy over the target region (tumor) defined by Bragg peak.

On the other hand, in order to improve treatment quality in carbon ion therapy, the dose adjustment is very important. It requires better understanding of carbon fragmentation in the body. Since carbon ions are fragmented into a large number of secondary ions, which cause unwanted dose beyond the tumor area. There were recent activities in order to measure the carbon fragmentation using nuclear emulsion techniques. In this work, a Geant4 based simulation of carbon fragmentation has been done using nuclear emulsion films interleaved with lexan layers as tissue equivalent medium. We have performed Data/MC comparisons using four different fragmentation models in Geant4.

REFERENCES

- [1] [http://newscenter.lbl.gov/feature stories/2010/10/18/ion-beam-therapy/](http://newscenter.lbl.gov/feature%20stories/2010/10/18/ion-beam-therapy/) Retrieved May 25, 2012.
- [2] <http://three.usra.edu/articles/AndoCarbonIonRadiotherapy62510Chap3> Retrieved May 20, 2012.
- [3] E. Haettner, *Experimental Study on Carbon Ion Fragmentation in Water using GSI Therapy Beams*, KTH university, April 2006.
- [4] [http://hypernews.slac.stanford.edu/HyperNews/geant4/get/phys-list.html ?inline=1](http://hypernews.slac.stanford.edu/HyperNews/geant4/get/phys-list.html?inline=1) Retrieved May 21, 2012.
- [5] <http://geant4.cern.ch/support/index.shtml> Retrieved June 1, 2012.
- [6] <http://geant4.cern.ch/support/userdocuments.shtml> Retrieved June 5, 2012.
- [7] <http://geant4.slac.stanford.edu/installation/> Retrieved June 5, 2012.
- [8] [http://geant4.web.cern.ch/geant4/G4UsersDocuments /UsersGuides/ For Application Developer/html/GettingStarted/particleDef.html](http://geant4.web.cern.ch/geant4/G4UsersDocuments/UsersGuides/ForApplicationDeveloper/html/GettingStarted/particleDef.html) Retrieved June 5, 2012.
- [9] [http://geant4.web.cern.ch/geant4/UserDocumentation/UsersGuides/ForApplication Developer/html/ch04.html](http://geant4.web.cern.ch/geant4/UserDocumentation/UsersGuides/ForApplicationDeveloper/html/ch04.html) Retrieved June 6, 2012.
- [10] A. Heikkinen, *GEANT4 Hadronic Cascademodels and CMS Data Analysis*, Helsinki Institute of Physics, University of Helsinki, Finland, P.O. Box 64, FIN-00014 ,2009.
- [11] [http://geant4.cern.ch/reports/talks/ivanchenko instrumentation](http://geant4.cern.ch/reports/talks/ivanchenko%20instrumentation) Retrieved June 6, 2012.
- [12] Tatsumi Koi, et al., Wright, *Validation of Hadronic Models in Geant4*, Stanford Linear Accelerator Center, Menlo Park, California, USA, SLAC-PUB-12836, 2009.
- [13] Tatsumi Koi, *New native QMD code in Geant4* Presentation, SLAC National Accelerator Laboratory, Tokyo 2010.

- [14] http://geant4.slac.stanford.edu/Space06/presentations/01_Monday/08-Koi_ValidationAndDevelopmentPlanOfGeant4IonPhysics Retrieved June 6, 2012.
- [15] http://geant4.cern.ch/support/proc_mod_catalog/models/hadronic/G4WilsonAbrasionModel.html Retrieved June 6, 2012.
- [16] http://www.dkfz.de/en/medphys/heavy_ion_therapy/index.html Retrieved June 10, 2012.
- [17] http://www.dkfz.de/en/medphys/appl_med_rad_physics/Heavy_ion_therapy.html Retrieved June 10, 2012.
- [18] <http://www-bd.fnal.gov/ntf/reference/hadrontreat> Retrieved June 14, 2012.
- [19] D. Cussol, *Nuclear Physics and Hadrontherapy*, University of Caen Basse-Normandie, 2011.
- [20] http://www.cancer.net/patient/All Cancer/Cancer.Net_Feature_Articles/Treatments Tests and Procedures/Explaining Proton Therapy Retrieved June 14, 2012.
- [21] <http://www.cancer.gov/cancertopics/factsheet/Therapy/lasers> Retrieved June 14, 2012.
- [22] <http://www.slideshare.net/ajjitchandran/electron-beam-therapy> Retrieved June 14, 2012.
- [23] <http://www.aapm.org/meetings/03SS/Presentations/Hogstrom>, Retrieved June 14, 2012.
- [24] <http://geant4.slac.stanford.edu/tutorial/mcgill06/Kernel1> Retrieved May 20, 2012.
- [25] T. Toshito, et al., *Measurements of projectile-like 8Be and 9B production in 200–400 MeV/nucleon ^{12}C on water*, Japan Science and Technology Agency, 10.1103/PhysRevC.78.067602, 2009.
- [26] G. De Lellis, et al, *Measurement of the fragmentation of Carbon nuclei*, Nuclear Physics A 853, 124–134, 2011.
- [27] Leo.W.R. *Techniques for Nuclear and Particle Physics Experiments*, Second revised edition, Published 1994.

[28] R.C.Fernow. *Introduction to Experimental Particle Physics*, Cambridge university, Published 1986.

[29] M. Regler. *Medical Accelerators for Hadrontherapy with Protons and Carbon Ions* . Institute of High Energy Physics of the Austrian Academy of Science, Vienna 2CERN, Geneva 23 7 June 2002.

[30] H. Suit. *Proton vs carbon ion beams in the definitive radiation treatment of cancer patients* Department of Radiation Oncology, Boston, MA, USA Radiotherapy and Oncology 95 3–22 2010.